Chem. Chem. Technol., 2024,
Vol. 18, No. 1, pp. 57–65

Chemical Technology

EXPERIMENTAL EVALUATION OF AN EMPIRICAL EQUATION IN A GASEOUS FLOW

***Arlitt Amy Lozano Povis*[1,✉], *Elías Adrián Sanabria Perez*[1]**

https://doi.org/10.23939/chcht18.01.057

Abstract. In this paper, the estimation error of Dr. Pole's empirical equation was evaluated using copper pipes of different diameters (0.00953, 0.0127, 0.01588 m), under different flow pressure conditions (0, 300, 500, 1000, 1500, 2000, 2500, 3000 L/h). To carry out the experiments, the following instruments were used: an air compressor, 2 flow valves, a needle valve, a gas rotameter, copper piping, pressure gauges and transmitters, a Norus data logger with 4 to 20 mA output signals, thermocouples, and thermoresistors. They allow us to establish that the air pressure drops when the flowing through the pipes is higher (380 Pa) for small diameter pipes (0.00953 m), compared to larger diameters (0.01270 m and 0.01588 m) with a maximum of 54 and 28 Pa, respectively; and in relation to the flow rates, the pressure drop increases with a quadratic trend with respect to the flow rate. Finally, the residual errors that the empirical equation has in the pressure drop calculations, in general terms, are not of great magnitude.

Keywords: airflow, flow, pressure, diameter, pipe.

1. Introduction

In the oil and natural gas industry, there are internal corrosion problems that can be the cause of multiple accidents in the facilities where these activities are carried out,[1] drastically reducing their useful life and production volumes, ultimately leading to a decrease in the profitability of oil and gas production.[2] Thus, when water is transferred in this state and combined with these hydrocarbons, alterations in both gaseous and liquid flow patterns can be caused, as well as mass transfer rates that can accelerate the corrosion of the metallic surfaces of the pipes.[3] Therefore, the selection of pipe material grades with higher corrosion resistance and the treatment of the circulating water have been considered as preventive measures.[4]

In the specialized literature, empirical equations such as those of Darcy Weisbach, Colebrook-White, Renouard, Weymouth, Cox, and others, have been identified; whose purpose is to provide the methodology to follow to estimate the pressure drop of gas flows. Likewise, and as the basis for this study, we highlight the empirical equation of Dr. Pole, in which the gas flow rate, as well as the pipe diameter and length, are related to the pressure loss. An unknown aspect of this equation is the accuracy or error it has in its estimates.[5]

Some studies have shown that the change in variables such as gas pressure, confining pressure, and effective pressure can affect the gas permeability of rocky materials such as (sandstone, coal, etc.).[6]

In addition, the increase in the gas flow will generate a reduction in the gas temperature and the density of its electrons, affecting the residence time of both heavy particles and electrons.[7]

Therefore, the equations applied in these case studies must be the ones that describe the flow phenomenon under the conditions of a given situation best of all, so that, with the calculations, the pipes that meet the requirements can be selected. necessary for the installation of pipe networks that carry gas.

Thus, in this project, it is proposed to evaluate the mentioned equation with experimental data, to verify the error that it has, in the estimation of the pressure loss using air as the fluid that circulates through straight pipes, at low pressures. In addition, this study will allow to spread and understand the pressure drop of a compressible fluid in copper pipes of different diameters. It is important to know that the model obtained can serve as a basis for the design of gas networks of similar characteristics, industrial or commercial (pressure higher than 7000 Pa, model proposed by Muller) or for commercial networks (pressures lower or equal to 7000 Pa, Pole's model). This allows pressure losses to be calculated, to evaluate the functionality and feasibility of the design, and to systematize the total length of the pipe, the flow rate, and the gas speeds in the pipeline.

[1] Universidad Nacional del Centro del Perú, Facultad de Ingeniería Química
Mariscal Castilla 3909, Huancayo, Perú
✉ *lozanopovisarlitt@gmail.com*

2. Materials and Methods

The methodology adopted in this research consisted of carrying out experimental tests of airflow through copper pipes of different diameters and at different flow rates. In the tests, geometric data of the pipe, and thermodynamic properties (pressure and temperature of the air that enters and circulates) were collected. Finally, with the experimental data, a quadratic regression analysis of the pressure drop as a function of the flow was carried out and corrected to standard conditions to verify if they have a tendency or meet this condition, such as the equation proposed by Dr. Pole.

2.1. Laboratory Phase

The parts that compose it according to the scheme are:

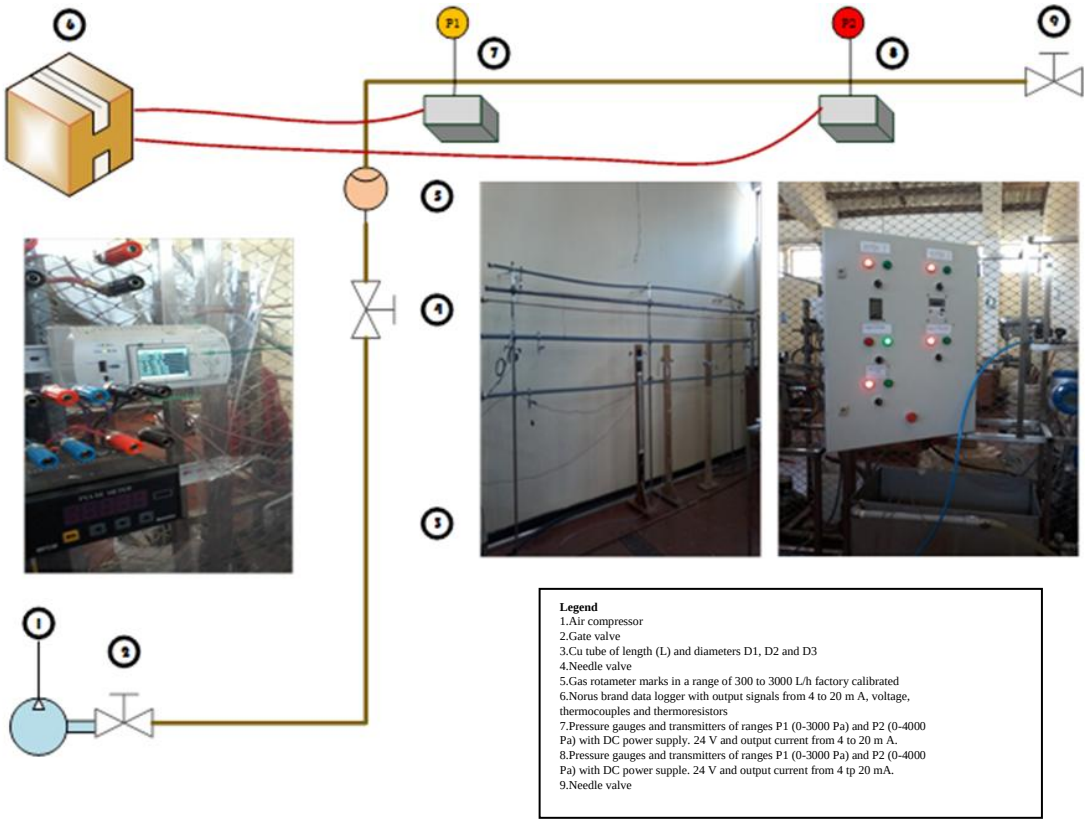

Fig. 1. Module diagram

1. An air compressor supplies this gas at a pressure ranging from 103421 to 344738 N/m². It has an automatic pressure control system to activate and deactivate the compressor motor.

2. A ball-type shut-off valve of ½ inch nominal diameter, to open or close the passage of air from the compressor to the copper pipe.

3. High-pressure hose with an external diameter of 0.10 m, which allows air to be transported from the compressor to the copper pipe.

4. 0.00635 m needle valve, which allows to formulate the flow and pressure of air that enters the rotameter and a copper pipe.

5. Gas rotameter, which allows the volumetric flow of air to be measured. Range from 300 to 3000 L/h. Made of glass and steel material. The diameters of the threads for the installation of the air inlet and outlet pipes are 0.00635 m.

6. Rigid copper tube type L, adapted at two points for pressure measurement, as well as for installation and removal inside the module. The points for pressure measurement are one from the other at a distance of 4.76 m. in the three tubes used in the tests (nominal external diameters: 0.01 m, 0.013 m, and 0.016 m)

7. Pressure gauges and transmitters. The range of the first one, which is located after the rotameter, is from 0 to 4000 Pa and the second one, which is at the end, is from 0 to 3000 Pa. The electrical signal transmitted by both is from 4 to 20 mA.

8. NORUS brand data logger and indicator. It allows visualizing the magnitude of the pressure measu-

rements. The input type of electrical signals is universal. It has 8 channels for the connection and detection of analog signals.

9. This module allows you to exchange pipes of different materials and diameters (up to approximately 1-inch nominal diameter). It also allows experiments to be carried out with different gaseous fluids (air, liquefied propane gas, natural gas, O_2, N_2, and CO_2) at low pressures. For high pressures, it is necessary to replace the pressure gauges to an appropriate range.

2.2. Experimental Procedure

To carry out the experimental tests, the 0.010 m diameter Cu pipe was installed for the first experiment. Then, the high-pressure hose was connected to the compressor and it was verified that it is in perfect working order; while simultaneously the data recording an indicator came on, verifying that all the equipment works correctly. As an additional step, it must be avoided that, when turning on the air compressor, the registered flow rate is greater than 4000 Pa and that the high-pressure hose is properly connected. Then, the temperature must be measured when the flow registers a value of zero, as well as the pressure data at P1 y P2. Another important aspect is to regulate the flow of the rotameter according to the estimated time for each experiment (300, 500, 1000, 1500, 2000, 2500, and 3000 L/h).

Once work was finished with the first pipe and after recording the pressure data correctly, the next pipe was connected to the data recording indicator, repeating the procedure described above. Finally, after performing all the measurements, the equipment was disconnected.

2.3. Cabinet Phase

This equation allows us to determine the pressure loss in the gaseous flow at pressures less than 7000 Pa. Its importance is explained in Fig. 2.

Then the equation provided in the NTP 111.01[8] is the following:

$$D = \Phi = \sqrt[5]{\frac{L}{\Delta P} \times \frac{PCT}{Coefficient \times K_1}^2} \quad (1)$$

where $D = \Phi$ is the actual inner diameter (m); L is the length (m); ΔP is the pressure loss (Pa); PCT is the total calculation power (J/s) and K_1 is the friction factor according to Φ (Table 1).

Rearranging Eq. (1) to make it explicit for pressure drop we have:

$$\Delta P = \frac{PCT}{coef^2 \times {K_1}^2} \times L \times \frac{1}{D^5} \quad (2)$$

The total calculation power is a function of the volumetric flow of the gas that circulates through a pipe, which leads it to one or several pieces of equipment that consume fuel gas to release heat by combustion. This term is related to the volumetric flow as follows (Calculation of gas installations).

$$PCT = Q \times PCS \quad (3)$$

Where, Q is the flow rate (L/h); PCS= Higher calorific value (J/m^3)

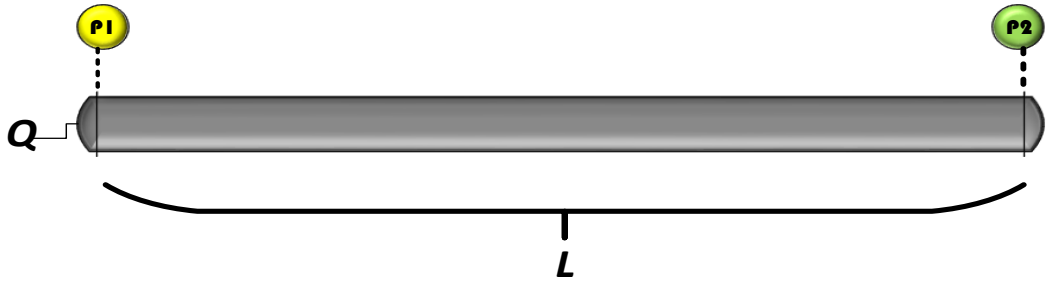

Fig. 2. Scheme of pressure drop in the pipe

Table 1. The coefficient for Natural Gas

Φ	**K_1**
$0.009525 - 0.0254$	1800
$0.03175 - 0.0381$	1980
$0.0508 - 0.0635$	2160
0.0762	2340
0.1016	2420

Source: [8]

Then substituting Eq. (3) in Eq. (2) and ordering we have:

$$\Delta P = \frac{PCS^2}{coef^2 \times {K_1}^2} \times L \times \frac{Q^2}{D^5} \quad (4)$$

In this last equation, the superior calorific value and the coefficient depend on the physical characteristics of the gas that circulates for the pipe, while K_1 depends only on the diameter of the pipe.

Observation:

The higher heating value of a gas is the amount of energy released by the complete combustion of a unit volume of a gas under normal conditions of P and *T* (273.15 K and 101325 Pa). This energy released is total, a part of which goes so that the water that is produced in the combustion changes the phase from liquid to vapor, there is also a lower calorific value.

Eq. (4), expressing it for any gas, would have the form:

$$\Delta P = K_{GAS} K_{TUBE} \times L \times \frac{Q_2}{D^5} \quad (5)$$

From another specialized source, Pole's equation has the form:

$$\Delta P = K_2 L Q^2 = K_3 Q^2 \quad (6)$$

K_2 is a constant that depends on the type of gas, the installation material and the diameter of the pipe.

Eqs. (5) and (6) have similar forms, the only difference is that the constants K_{gas}, K_{tube} and D are grouped into a single K_2.

For this investigation, Eq. (6) will be used, which is expressed in general terms with separate constants for the gas and the tube.

In the case of calculating the corrected flow rate, we deduce the following Eq. (7) at standard conditions:

$$T = 298.15\ K\ , P = 101325\ Pa$$

$$Q_{\text{corrected } T,P} = Q_{exp}\ T, P\ \times \frac{P_{exp}}{P_{Correc}} \times \frac{T_{correc}}{T_{exp}} \quad (7)$$

2.4. Calculation Procedure

2.4.1. Flow Rate at Standard Conditions

With the data obtained from the flow rate experiments, pressure at point 1, and air temperature, the calculation of the flow rate at standard conditions (298.15 K and 101325 Pa) was carried out using Eq. (6) that relates to the experimental flow rate, the experimental pressure at 69306.3 Pa, the absolute pressure of 101325 Pa, temperature of 298.15 K and air temperature.

2.4.2. Obtaining the Coefficient K_3

From Eq. (5) and applying the polynomial regression method, the correlation coefficients representing the coefficient K_3 were obtained that later will be used to obtain the quadratic regression curve.

2.4.3. Calculation of K_{tube}

From Eq. (4) and with the data obtained from the relative density of the air, the coefficient K_3 and knowing the diameter of the pipes thaw areas and the length recorded between points P_1 and P_2, determined the K_{tube}.

3. Results and Discussions

The experimental data shown in Tables 2 and 3 are the characteristics of the tubes and air flow data, gauge pressures at the two points of the copper pipes and the air temperature.

All the tubes used were copper, rigid, and type L.

The flow rate was regulated with the needle valve and measured with the rotameter, at temperature and pressure conditions (*P*1) that are recorded in this table. The air temperature measurement was made at the outlet of the copper pipe, and it was considered that the variation in air temperature when it circulates from the rotameter to the outlet of the pipe is insignificant. Also, it was considered that the air pressure drop from the rotameter to the first pressure point (*P*1) is negligible. These considerations were applied to correct the air flow from the experimental conditions, to the standard pressure and temperature conditions (298.15 K and 101325 Pa).

3.1. Pressure Drop and Flow Rate

This section contains Table 4, which shows the results of the calculations: flow rate at standard conditions, the relative density of air at the experimental conditions, and the pressure loss observed in each experiment. It is observed in the data that the relative density of the air is less than unity since the gauge pressure in the place where we carried out the experimental tests is less (69306.3 Pa) than the atmospheric pressure at sea level.

Table 2. Characteristics of the tubes

N°	External diameter (m)	Wall thickness (m)	Internal diameter (m)	Length between pressure measurement points (m)
1	0.00953	0.00076	0.00801	4.76
2	0.01270	0.00086	0.01092	4.76
3	0.01588	0.00102	0.01384	4.76

Table 3. Measurements of air flow, pressures, and temperature

N°	FLOW (L/h)	Outside Diameter Tube = **0.00953 m**			Outside Diameter Tube = **0.0127 m**			Outside Diameter Tube = **0.01588 m**		
		P_1 (Pa)	**P_2 (Pa)**	**T° (K)**	**P_1 (Pa)**	**P_2 (Pa)**	**T° (K)**	**P_1 (Pa)**	**P_2 (Pa)**	**T° (K)**
1	0	0.000	0.000	293.15	0.000	0.000	293.15	0.000	0.000	293.15
2	0	0.000	0.000	293.15	0.000	0.000	293.15	0.000	0.000	293.15
3	0	0.000	0.000	293.15	0.000	0.000	293.15	0.000	0.000	293.15
4	300	137.0	3.2	293.15	43.8	1.5	295.15	14.2	1.3	293.15
5	300	141.0	3.5	293.15	43.7	1.4	293.15	13.1	1.2	293.15
6	300	137.4	3.3	292.15	43.7	1.3	293.15	14.9	2.1	293.15
7	500	199.6	3.5	293.15	61.7	2.1	294.65	19.9	3.1	293.15
8	500	197.4	3.5	293.15	63.4	2.3	293.15	20.4	2.4	293.15
9	500	199.3	3.6	292.65	63.5	2.3	293.15	21.6	2.9	293.15
10	1000	668.1	15.3	293.15	122.8	4.9	294.15	42.2	10.3	293.65
11	1000	663.7	16.0	293.15	122.7	4.6	293.15	45.2	07.9	293.15
12	1000	681.9	16.7	292.65	125.2	4.4	293.15	46.1	10.9	293.15
13	1500	1222.7	28.8	293.15	317.2	11.4	294.15	83.8	19.7	293.65
14	1500	1286.6	30.7	293.15	315.6	11.4	293.15	76.4	16.5	293.15
15	1500	1285.8	30.6	293.15	318.5	13.9	293.15	81.3	20.1	293.15
16	2000	2021.5	47.8	293.15	512.1	18.6	293.65	155.3	26.4	293.15
17	2000	2038.8	49.8	293.15	528.9	22.3	293.15	152.2	35.3	293.15
18	2000	2065.5	49.2	293.15	527.8	22.0	293.15	152.2	25.6	293.15
19	2500	2808.9	66.9	293.15	753.6	32.8	293.15	221.3	51.8	293.15
20	2500	2932.7	70.4	293.15	744.0	28.4	293.15	208.8	38.0	293.15
21	2500	2835.0	67.8	293.15	744.7	32.8	293.15	223.8	54.3	293.15
22	3000	4013.0	97.8	293.15	1072.3	42.2	293.15	300.7	76.6	293.15
23	3000	3787.1	97.5	293.15	1046.8	47.3	293.15	285.5	52.0	293.15
24	3000	3945.3	98.5	293.15	1069.1	47.4	293.15	295.5	54.5	293.15

Table 4. Calculation results for flow rate at standard conditions and relative air density

	FLOW (L/h)	Outside Diameter Tube = **0.00953 m**			Outside Diameter Tube = **0.0127 m**			Outside Diameter Tube = **0.01588 m**		
		Standard Flow (L/h)	**P_1-P_2 (Pa)**	**Relative density of air**	**Standard Flow (L/h)**	**P_1-P_2 (Pa)**	**Relative density of air**	**Standard Flow (L/h)**	**P_1-P_2 (Pa)**	**Relative density of air**
1	2	3	4	5	6	7	8	9	10	11
1	0	0.0	0.000	0.696	0.0	0.000	0.696	0.0	0.000	0.696
2	0	0.0	0.000	0.696	0.0	0.000	0.696	0.0	0.000	0.696
3	0	0.0	0.000	0.696	0.0	0.000	0.696	0.0	0.000	0.696
4	300	209.2	133.8	0.697	207.5	42.3	0.692	208.8	12.9	0.696
5	300	209.2	137.5	0.697	208.9	42.3	0.696	208.8	11.9	0.696
6	300	209.9	134.1	0.700	208.9	42.4	0.696	208.8	12.8	0.696
7	500	349.0	196.1	0.698	346.5	59.6	0.693	348.1	16.8	0.696
8	500	349.0	193.9	0.698	348.3	61.1	0.697	348.1	18.0	0.696
9	500	349.6	195.7	0.699	348.3	61.2	0.697	348.1	18.7	0.696
10	1000	702.7	652.8	0.703	694.8	117.9	0.695	695.2	31.9	0.695
11	1000	702.6	647.7	0.703	697.2	118.1	0.697	696.4	37.3	0.696
12	1000	704.0	665.2	0.704	697.2	120.8	0.697	696.4	35.2	0.696
13	1500	1062.3	1193.9	0.708	1045.1	305.8	0.697	1043.4	64.1	0.696
14	1500	1063.3	1255.9	0.709	1048.7	304.2	0.699	1045.1	59.9	0.697
15	1500	1063.3	1255.2	0.709	1048.7	304.6	0.699	1045.1	61.2	0.697
16	2000	1432.5	1973.7	0.716	1399.8	493.5	0.700	1395.0	128.9	0.697
17	2000	1432.8	1989.0	0.716	1402.5	506.6	0.701	1394.9	116.9	0.697
18	2000	1433.4	2016.3	0.717	1402.5	505.8	0.701	1394.9	126.6	0.697

Continuation of **Table 4**

1	2	3	4	5	6	7	8	9	10	11
19	2500	1810.4	2742.0	0.724	1758.8	720.8	0.703	1745.4	169.5	0.698
20	2500	1813.5	2862.3	0.725	1758.5	715.6	0.703	1745.1	170.8	0.698
21	2500	1811.0	2767.2	0.724	1758.5	711.9	0.703	1745.5	169.5	0.698
22	3000	2208.7	3915.2	0.736	2120.1	1030.1	0.707	2096.9	224.1	0.699
23	3000	2201.9	3689.6	0.734	2119.3	999.5	0.706	2096.4	233.5	0.699
24	3000	2206.6	3846.8	0.735	2120.0	1021.7	0.707	2096.7	241.0	0.699

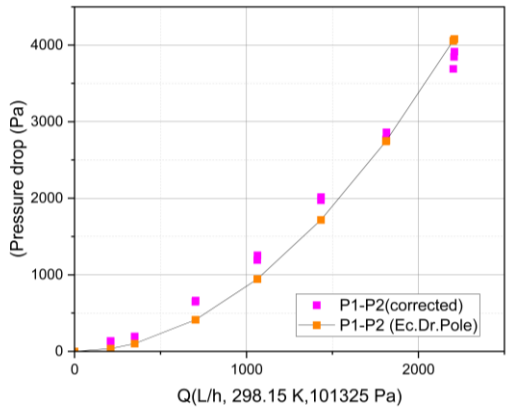

а

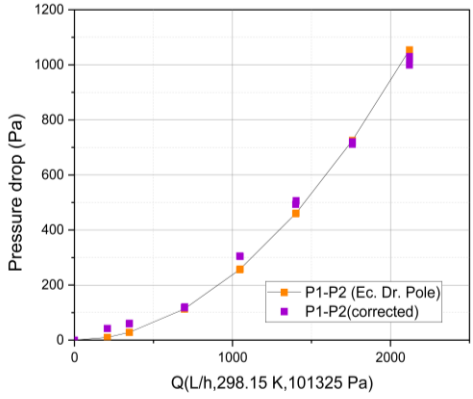

б

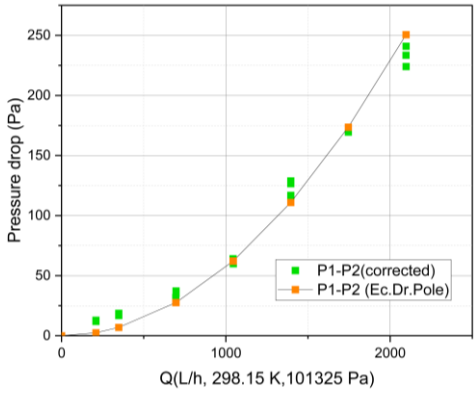

c

Fig. 3. Pressure drop vs. air flow rate at standard conditions, a) 0.00953, b) 0.0127, c) 0.01588 m external diameter copper tubing

Visualizing these data graphically (Fig. 3), it can be seen that the pressure drop experienced by the air when it travels a length of 4.76 m through the copper pipes increases with the air flow. Likewise, the trend curves are made with the quadratic equations according to the form proposed by Dr. Pole (Eq. (3)). The comparison of the experimental data with those of the trend line equation shows, in all three cases, that the increase in pressure drop as a function of flow rate has a trend that approximates the quadratic equation without an independent term that Dr. Pole proposes.

The standard flow rate used in Fig. 3 is less than the flow rates measured at the experimental conditions (Fig. 4). The reason for this is the difference in atmospheric pressure, as well as in the temperatures. If the three figures above are superimposed into one, it is found that the pressure drop in 4.76 m of copper pipe is greater when the diameter is small.

3.2. Coefficients of Dr. Pole's Equation

The calculated empirical coefficients are shown in Table 6. The empirical coefficient K_3 was calculated, according to Eq. (5). This value was obtained by a polynomial regression for the set of experimental data obtained in each pipe. In addition, it is worth mentioning that, for the regression, the form of the equation that was adopted was of the second degree as a single term (without an independent term and neither a first-degree term).

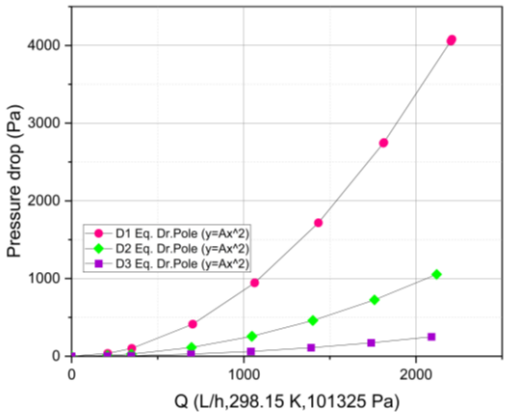

Fig. 4. Graphical representation of the pressure drop vs. the air flow rate at standard conditions, for the three copper pipes

From the calculations, the correlation coefficient was also obtained for each analyzed equation. Finally, the average coefficient K_1 is presented in this Table for each equation according to Eq. (4). For this, it is being considered that $K_1 = K_{tube}$, and in the calculations it was considered that K_{GAS} is equal to the relative density of air, similar to what happens with the Renouard equation.

3.3. Residual Errors of Dr. Pole's Equation

Next, the residual errors of the Pole equation for the three pipes are graphically observed. This error was calculated by the difference of the experimental pressure drop, with respect to those obtained with those of Dr. Pole's equation, as shown in Fig. 5.

From the results of the pressure drop that was observed in the three cases, they lead to establish that this increases with small diameters. That is, there will be a greater drop in air pressure when the diameter of the pipe is small. In addition, it can be noted that the tendency of the pressure drop concerning the flow is that it approaches a quadratic equation, as proposed by Dr. Pole's equation, and that the results are similar to those reported by Badie et al.[9] Due to the retention and pressure gradient data for air-water and air-oil flow in a horizontal pipe of 0.079 m in diameter, if the liquid flow is increased, no matter how insignificant it may be, it causes an increase in the pressure gradient compared to a single-phase gas flow. While, Wu et al.[10] reported that the contact angle has little impact on the gas pressure drop for the stratified flow regime, but determines the meniscus of the two-phase interface, which affects the optical detection of liquid thickness in the experiment, resulting in the importance of understanding two-phase flow dynamics, multichannel design, experimental design, and control of two-phase flows in thin channels. As well, Liang et al.[11] analyzed the influence of parallel gas flow direction, velocity, and temperature on the non-isothermal liquid bridge flow structure using the PIV technique, to explain these flow patterns and to model pressure drop, rate of mass transfer, and the interfacial area for a 0.03 m diameter vertical tube, the operating conditions of which were at ambient pressure and temperature, registering values below 0.30-0.32. Likewise, the general equation proposed by Dr. Pole indicates that the pressure drop of gas at low pressures: a) varies directly and linearly with the length of the pipe, b) varies according to the function of the second degree concerning the flow and, c) it varies inversely according to the function of the fifth-degree with respect to the internal diameter of the pipe. According to this and the experimental results, the quadratic trend of the pressure drop can be verified. Also, the average empirical tube constant (K_{tube}) indicates that it varies according to the pipe being used, as found in the specialized literature. For example, Bissor et al.[12] developed the numerical simulation and subsequent experimentation of a flow composed of air and liquid, establishing new mechanical models that predict the effect of parameters such as gas pressure, diameter, and inclination of the system's piping on the critical gas flow rate necessary to remove the liquid of the piping system and thus prevent them from affecting the components of these systems where these activities are carried out. In addition, Alsaadi et al.[13] developed experiments with air and water in a 0.0762 m diameter pipe and with a good deviation of 60° to 88° from the vertical, in which the results showed a significant effect of the angle of deviation in the beginning of a load of liquid, in addition to the diameter of the pipe with which you worked.

Regarding the correlation coefficients that were obtained for each quadratic regression, they confirm that there is a second-degree trend of the flow with respect to the pressure drop since the values are very close to the unit. In this point, Zhou and Yuan[14] established that, in addition to gas velocity, liquid retention is an important variable, basing their research on the Turner droplet model; but that from his experiments he established a new model that showed a better correlation between these variables. Similar applications were made by Trifonov[15] for the theoretical analysis of a gas-liquid flow in favor of the current between two inclined plates, based on the Navier-Stokes equation, establishing that the gas flow significantly affects this variable and the phase velocity.

Table 6. Results of the empirical coefficients of Dr. Pole's equation and quadratic correlation coefficient

N°	EXTERNAL DIAMETER (m)	EQUATION OF DR. POLE ($\Delta P = K_3 Q^2$)	CORRELATION COEFFICIENT	AVERAGE COEFFICIENT K_1
1	0.00953	$8.35229 \times 10^{-6}\ Q^2$	0.988962218	0.0815
2	0.0127	$2.34579 \times 10^{-6}\ Q^2$	0.995370011	0.1088
3	0.01588	$5.56443 \times 10^{-7}\ Q^2$	0.992728096	0.0846

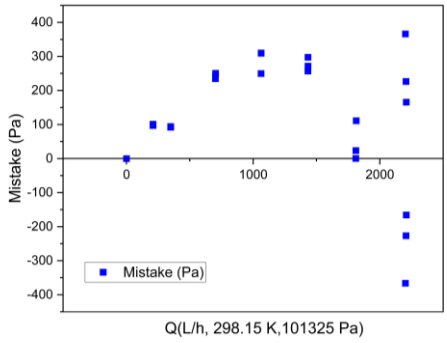

a

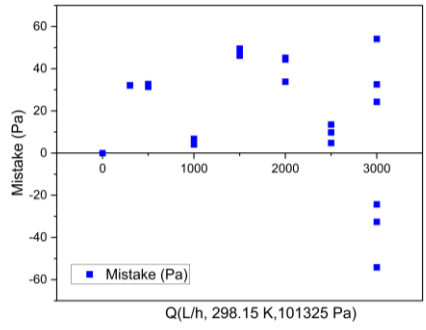

б

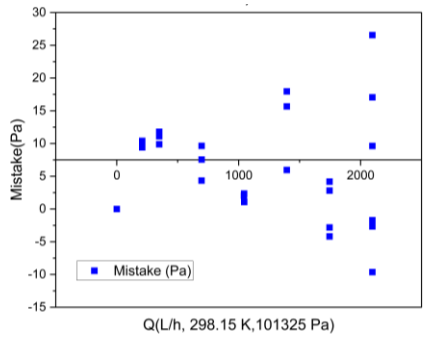

c

Fig. 5. Graphical representation of the residual errors as a function of the airflow rate at standard conditions, for a) 0.00953,b) 0.0127, c) 0.01588 m diameter pipe

The difference of the experimental pressure drop data concerning those obtained by Dr. Pole's equation; difference called a residual error, is greater in the pipe with an external diameter of 0.00953 m. reaching its maximum of 380 Pa, while for pipes with a diameter of 0.0127 m and 0.01588 m they are low, with maximums of 54 and 28 Pa, respectively. These differences can be reduced by installing a gas pressure regulator before the rotameter, so that the gas flow is stable, which in the experiments was done manually, and despite this, some variations affect the pressure measurements. But in general terms, the residual errors are small and do not have a particular trend with the air flow. In that sense, Shi et al.[16] pointed out that parameters such as the empty fraction are important to understand the flow of two phases in descending vertical pipes since there are models that have errors in the calculation of this variable when correlations are used, establishing a new model that takes into account the pattern of flow and which helps to overcome the deficiencies of conventional correlations. The relative errors which he obtained from these correlations ranged from 21.65% to 8.65%, and the mean absolute errors ranged from 8.57% to 23.17%, best fitting the experimental data. As well, Kopparthy et al.[17] established that in single-phase turbulent flows, the axial pressure change in the channel has been validated against experimental data and that only one of all the models was associated with flow regimes and air accumulations.

4. Conclusions

The errors that occur when using the empirical equation of Dr. Pole to calculate the pressure drop, are greater in small-diameter pipes compared to larger diameters and are not related to the air flow. Likewise, it was shown that the air pressure drop, when it circulates through a pipe, has a linear relationship with respect to

length, a second-degree relationship with respect to flow rate, and an inverse relationship with a fifth-degree function with respect to diameter. In addition, when it flows through pipes, it was shown that the highest rates occur when the diameters are smaller, compared to those with a larger diameter. About the flow rates, the pressure drop increases with a quadratic trend with the flow rate and the residual errors that the empirical equation has in the pressure drop calculations, in general terms, they are not of great magnitude. This equation is used to determine the pressure drop of air when it circulates through a pipe and has a linear relationship with respect to length, a second-degree relationship with respect to flow rate, and an inverse relationship with a fifth-degree function with respect to diameter.

References

[1] Song, G.; Li, Y.; Sum, A. K. Characterization of the Coupling between Gas Hydrate Formation and Multiphase Flow Conditions. *J. Nat. Gas Sci. Eng.* **2020**, *83*, 103567. https://doi.org/10.1016/J.JNGSE.2020.103567

[2] Pinchuk, S.; Galchenko, G.; Simonov, A.; Masakovskaya, L.; Roslyk, I. Complex Corrosion Protection of Tubing in Gas Wells. *Chem. Chem. Technol.* **2018**, *12*, 529–532. https://doi.org/10.23939/chcht12.04.529

[3] Paolinelli, L. D.; Nesic, S. Calculation of Mass Transfer Coefficients for Corrosion Prediction in Two-Phase Gas-Liquid Pipe Flow. *Int. J. Heat Mass Transf.* **2021**, *165*, 120689. https://doi.org/10.1016/J.IJHEATMASSTRANSFER.2020.120689

[4] Bannikov, L.; Miroshnichenko, D.; Pylypenko, O.; Pyshyev, S.; Fedevych, O.; Meshchanin, V. Coke Quenching Plenum Equipment Corrosion and Its Dependents on the Quality of the Biochemically Treated Water of the Coke-Chemical Production. *Chem. Chem. Technol.* **2022**, *16*, 328–336. https://doi.org/10.23939/chcht16.02.328

[5] Löhr, L.; Houben, R.; Moser, A. Optimal Power and Gas Flow for Large-Scale Transmission Systems. *Electr. Power Syst. Res.* **2020**, *189*, 106724. https://doi.org/10.1016/J.EPSR.2020.106724

[6] Xu, L.; Zhu, F.; Zha, F.; Chu, C.; Yang, C. Effects of Gas Pressure and Confining Pressure on Gas Flow Behavior in Saturated Cohesive Soils with Low Permeability. *Eng. Geol.* **2019**, *260*, 105241. https://doi.org/10.1016/J.ENGGEO.2019.105241

[7] Martínez-Aguilar, J.; González-Gago, C.; Castaños-Martínez, E.; Muñoz, J.; Calzada, M. D.; Rincón, R. Influence of Gas Flow on the Axial Distribution of Densities, Temperatures and Thermodynamic Equilibrium Degree in Surface-Wave Plasmas Sustained at Atmospheric Pressure. *Spectrochim. Acta Part B At. Spectrosc.* **2019**, *158*, 105636. https://doi.org/10.1016/J.SAB.2019.105636

[8] INDECOPI. *Gas Natural seco.Sistema de tuberías para instalaciones internas residenciales y comerciales.* https://www.italcaseperu.com/download/NTP 111.011 2006 Instalaciones internas residenciales y comerciales.pdf (accessed 2022-03-08).

[9] Badie, S.; Hale, C. P.; Lawrence, C. J.; Hewitt, G. F. Pressure Gradient and Holdup in Horizontal Two-Phase Gas–Liquid Flows with Low Liquid Loading. *Int. J. Multiph. Flow* **2000**, *26*, 1525–1543. https://doi.org/10.1016/S0301-9322(99)00102-0.

[10] Wu, J.; Li, Y.; Wang, Y. Three-Dimension Simulation of Two-Phase Flows in a Thin Gas Flow Channel of PEM Fuel Cell Using a Volume of Fluid Method. *Int. J. Hydrogen Energy* **2020**, *45* (54), 29730–29737. https://doi.org/10.1016/J.IJHYDENE.2019.09.149

[11] Liang, R.; Jin, X.; Yang, S.; Shi, J.; Zhang, S. Study on Flow Structure Transition in Thermocapillary Convection under Parallel Gas Flow. *Exp. Therm. Fluid Sci.* **2020**, *113*, 110037. https://doi.org/10.1016/J.EXPTHERMFLUSCI.2019.110037

[12] Bissor, E. H.; Yurishchev, A.; Ullmann, A.; Brauner, N. Prediction of the Critical Gas Flow Rate for Avoiding Liquid Accumulation in Natural Gas Pipelines. *Int. J. Multiph. Flow* **2020**, *130*, 103361. https://doi.org/10.1016/J.IJMULTIPHASEFLOW.2020.103361

[13] Alsaadi, Y.; Pereyra, E.; Torres, C.; Sarica, C. Liquid Loading of Highly Deviated Gas Wells from 60° to 88°. *Proc. - SPE Annu. Tech. Conf. Exhib.* **2015**, *2015-January*, 1752–1769. https://doi.org/10.2118/174852-MS

[14] Zhou, D.; Yuan, H. A New Model for Predicting Gas-Well Liquid Loading. *SPE Prod. Oper.* **2010**, *25* (02), 172–181. https://doi.org/10.2118/120580-PA

[15] Trifonov, Y. Y. Linear and Nonlinear Instabilities of a Co-Current Gas-Liquid Flow between Two Inclined Plates Analyzed Using the Navier–Stokes Equations. *Int. J. Multiph. Flow* **2020**, *122*, 103159. https://doi.org/10.1016/J.IJMULTIPHASEFLOW.2019.103159

[16] Shi, S.; Wang, Y.; Qi, Z.; Yan, W.; Zhou, F. Experimental Investigation and New Void-Fraction Calculation Method for Gas–Liquid Two-Phase Flows in Vertical Downward Pipe. *Exp. Therm. Fluid Sci.* **2021**, *121*, 110252. https://doi.org/10.1016/J.EXPTHERMFLUSCI.2020.110252

[17] Kopparthy, S.; Mansour, M.; Janiga, G.; Thévenin, D. Numerical Investigations of Turbulent Single-Phase and Two-Phase Flows in a Diffuser. *Int. J. Multiph. Flow* **2020**, *130*, 103333. https://doi.org/10.1016/J.IJMULTIPHASEFLOW.2020.103333

Received: September 09, 2022 / Revised: December 28, 2022 / Accepted: March 14, 2023

ЕКСПЕРИМЕНТАЛЬНА ОЦІНКА ЕМПІРИЧНОГО РІВНЯННЯ В ГАЗОВОМУ ПОТОЦІ

Анотація. *У цій статті оцінено похибку оцінювання емпіричного рівняння Пола з використанням мідних труб різних діаметрів (0,00953, 0,0127, 0,01588 м), за різних умов потоку (0, 300, 500, 1000, 1500, 2000, 2500, 3000 л/год). Для проведення експериментів були використані наступні прилади: повітряний компресор, 2 проточні вентилі, голчастий вентиль, газовий ротаметр, мідні трубопроводи, манометри і передавачі, реєстратор даних Norus з вихідними сигналами від 4 до 20 мА, термопари і терморезистори. Це дало змогу встановити, що падіння тиску повітря під час проходження через труби є вищим (380 Па) для труб малого діаметру (0,00953 м) порівняно з трубами більшого діаметру (0,01270 м і 0,01588 м) з максимальним значенням 54 і 28 Па, відповідно; і відносно швидкості потоку падіння тиску зростає з квадратичною тенденцією відносно швидкості потоку. Нарешті, залишкові похибки, які має емпіричне рівняння в розрахунках перепаду тиску, у цілому, не є великими.*

Ключові слова: *повітряний потік, витрата, тиск, діаметр, труба.*